Analysis of the coupled effect of steel studs and surface emissivity on internal insulation systems performance

Marco Manzan*, Amedeo Pezzi, Ezio Zandegiacomo De Zorzi

Department of Engineering and Architecture, University of Trieste, via A. Valerio 10, 34127 Trieste, Italy

ARTICLE INFO

Accepted 10 October 2019

Keywords:
Heat exchange
Internal insulation
Low-e surfaces
Refurbishment
Steel studs

ABSTRACT

Many kinds of insulation systems have been developed and applied over the years to all the constructive elements of the building, but the two most used strategies remain the external and internal insulation of vertical walls. However, about the latter often a significant issue is neglected: the overestimation of the thermal performance by disregarding the contribution of construction elements. Usually a uniform stratigraphy of the wall is considered and the evaluation of the performance of a non-uniform one leads to erroneous results about the overall behavior of the system. In this paper, we developed a different approach considering the presence of the steel studs used to attach this package to the existing wall and their influence on the thermal behavior of the structure. Through both experimental and numerical analysis, the possible application of low-e sheets inside the air cavity in various configurations and with different thicknesses of insulation is also taken into account. Results showed that neglecting the presence of the steel studs leads to an erroneous evaluation of the conductance of the refurbished wall with errors reaching up to 28.0% in low-e high-insulated cases. This work highlights how careful the designers have to be when using standard formulas to compute the thermal resistance of internal insulation wall systems.

1. Introduction

In the last decades, it has become more and more evident that building climatization constitutes a large, and very important, part of energy consumption in industrialized countries. Because of this, both researchers and regulations aimed to increase the thermal efficiency of the buildings to reduce energy usage. A wide set of solutions has been developed such as the application of external or internal insulation layers, the adoption of high-performance windows, the improvement of plant efficiency and exploitation of renewable resources. If some of these interventions are considered very valuable in terms of performance others, like the internal insulation of walls, are reputed problematic because of some critical issues. Considering the latter solution, the two main problems detected are the possibility of mold formation at the interface between the insulating panels and the structural layer of the wall and the loss of livable space due to the presence of an additional internal insulating layer. The latter problem leads to the development of methods for increasing thermal resistance allowing low-thickness layers.

In a number of cases the internal insulation system presents air gaps, therefore one way to increase the thermal performance is to reduce the radiative heat exchange in the air cavity. Low emissivity thin layers are usually applied to one or both the surfaces of the air cavity; therefore, many studies have been carried on to evaluate the beneficial effects of low-emission systems. Baldinelli [1] studied the effect of a reflective panel inserted in the middle of the air gap of a vertical wall, thus creating two separated cavities both having one low-e surface and increasing the overall thermal resistance of the interspace. Obviously, the operating conditions of a low-e solution are very important; in fact, it has been proved [2] that as the temperature difference between the surfaces of air cavity increases, the importance of surface thermal emissivity grows.

Other classical analysis parameters like geometrical dimensions, internal loads' entity, air ventilation rate and climatic data influence the performance of a low-e solution. As an example, Saber [3] conducted a parametric study to investigate the effect of inclination angle, foil emissivity and direction of the heat flow on an isolated air cavity inside a shell structure. He evidenced that by decreasing the foil emissivity from 0.90 to 0.05 in a configuration with horizontal structure and downward heat flow, typical of a summer season roof case, the structure's R-value increases by 26.10%. Considering the same solution with an upward heat flow,

* Corresponding author.
E-mail address: manzan@units.it (M. Manzan).

as in a winter season roof case, the R-value increased by 8.90%. With an inclination of 30°, the decrease of emissivity led to an increment of R-value of 17.65% and 10.50% for downward and upward heat flux respectively.

Similar studies were conducted by Fantucci et al. [4] focusing on building roofs with ventilated air cavity and low emissivity foils or paints. They demonstrated that with the insertion of reflective paint or aluminum foil the indoor summer heat gains decreased by a value ranging between 10.00% and 53.00%.

Ibrahim et al. [5] developed a numerical simulation that demonstrated the correlation between different thicknesses of insulation and surfaces' emissivity in determining the energy savings in a building. The paper highlighted that with high levels of insulation the influence of surfaces' emissivities becomes nearly negligible.

In another study Joudi et al. [6] using experimental tests and a CFD model, compared the performance of conventional internal and external insulation systems against solutions featuring low-e layers; the former with only an internal low-e surface, the latter with both internal and external additional low-e insulations. Basing their studies on Stockholm climate data, they proved that for the low-e internal insulation case the increase of building dimensions, while maintaining unchanged all other parameters of the model, led to a slight reduction of the obtained energy savings. However, in both low-e cases the increase of internal loads led to a reduction of the total performance of the cabin, since winter heating savings where heavily counterbalanced by the incapacity of the system in dissipating the heat during summer season. On the other hand, an increase of air ventilation rate led, with different behaviors, to a performance improvement for both low-e solutions. The study proved that an internal low-e package is better suited for colder climates while an exterior one works well in warmer environment while a two-side low-e solution is best suited for mild climates.

An additional aspect to consider when dealing with low-e sheets is the possible emissivity change due to various causes like material oxidation and accumulation of dust or vapor on the surface. Cook et al. [7] conducted experiments showing that the accumulation of dust on horizontal low-e sheets increased their emissivity from an initial value of 0.05 to a maximum value ranging from 0.67 to 0.85, depending on the type of dust.

Despite the great amount of studies dealing with low-e wall insulation systems, no extensive information is available in literature about the overestimation of the thermal performance of the internal insulation packages applied to massive constructions. This issue happens because, when computing the thermal performance of the structure, the presence of metal studs needed to attach to the existing wall the plasterboard panels, used as internal finishing layer, usually it is not taken into account. However, the studs are fixed to the underneath wall and can lead to the formation of thermal bridges.

However, his problem is well known in light frame and light steel frame constructions; for example, Kosny et al. [8] numerically analyzed various metal frame walls' configurations pointing out the difference between clear wall and frame R-values. In another study, De Angelis et al. [9] displayed the necessity of using numerical methods to obtain the correct U-value of light frame walls and discouraged the application of simplified calculation methods. Another work [10] explained the problem related to heat exchange in such structures and how thermal bridges created by metal studs affect the whole system.

Regarding massive constructions, Manzan et al. [11] studied the effect of structural elements with internal compact insulation without air gaps. They used simplified methods to compute the overall conductance of the insulated wall; the results showed that the conductance of the system was 6.60% higher for wooden studs and 32.80% higher for metal studs if compared with the clear wall values.

In a successive work [12] the metal studs case was studied by Manzan et al. using numerical techniques. They highlighted the influence of the steel studs on the total performance of an internal insulation wall package. They proved that the correct evaluation of the whole insulation system displayed a mean conductance 20% higher than the one computed using the one-dimensional clear wall values.

However, alternative solutions consider the creation of air gaps in the insulation package, in this case the combined effect of steel studs and surfaces with low values of emissivity has not been studied before. This effect could lead to an erroneous evaluation of the performance of insulation systems featuring also low-e layers in internal air gaps. This effect leads to a possible overestimation of energy reduction in refurbished buildings.

2. Aim of the study

The aim of this study is to evaluate the impact of the presence of steel studs inside the air cavities on the overall system performance for internally insulated massive structures. Indeed, structural studs are always needed to fix plasterboards to the wall in a typical internal insulation package, however they worsen the overall performance of the internal insulation system. An additional objective is to evaluate the possible improvement that the application of low-e sheets could have on the system performance and the interaction between metal studs and low-e layers. The analysis has been carried on for different thicknesses of the insulation layer, ranging from 3 cm to 8 cm in order to take into account various levels of insulation.

3. Experimental study

To effectively consider the influence of the steel studs in this kind of insulation, experimental tests have been conducted at Edilmaster building school in Trieste. Inside a controlled laboratory, a reproduction of a typical massive wall used in historical buildings has been realized. The wall has been provided with an internal insulated system to replicate a refurbishment activity on an existing building. The experimental setup has been already presented in [11] and it consists in two cells maintained at constant different temperature separated by a specimen wall. Electrical resistances heat up the hot chamber, while a refrigerator unit cools down the other one.

The test cell is 4.70 m long, 2.24 m wide and 2.20 m tall; the tested wall has dimensions of 1.90×1.93 m for a total area of 3.67 m^2. The specimen consists in a massive brick wall 0.51 m wide with plaster layers on each side. The internal insulation system consists of an insulation layer 3 cm thick, an air gap of 3 cm, and 1.25 cm thick plasterboard panels as reported in Fig. 1a.

To fix the plasterboard panels to the wall, vertical C-shaped 0.60 mm thick steel studs were placed at a distance of 56 cm each other as presented in Fig. 1a. The C-shaped 6×3 cm metal studs are fixed in place by two metal clamps, 6 cm wide each, fixed to the underneath wall. The stiffness of the structure is obtained through U-shaped 3×3 cm metal profiles located at the top and bottom of the tested wall.

Measures of the main parameters were carried on through a heat flow meter BSR240 and four thermal resistances BST124, while to set up the correct thermal conditions in the two chambers, room temperature sensors were used. The measured outputs were then collected and used to compute the thermal conductance.

A pool of experiments has been conducted in stationary conditions; the two most important tests were the one with normal surface emissivity, from now on referred as Case 1, and one with

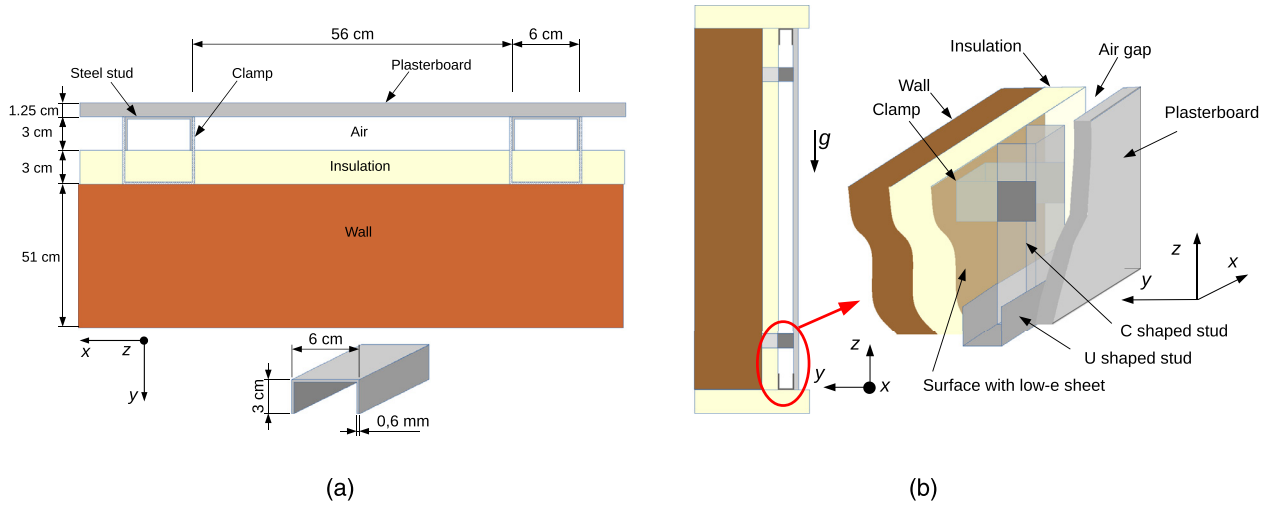

Fig. 1. internal insulation layer composition (a), detail of the fixing system (b).

Table 1
Conductance experimental results.

	C_{CW} [W/(m^2 K)]	C_{st} [W/(m^2 K)]
Case 1	0.59	/
Case 2	0.38	0.82

the insertion of an aluminum foil on the insulating layer side of the air cavity, from now on referred as Case 2. Measures of the heat flux were taken at the center of the plasterboard, representing clear wall values, and in correspondence of the steel studs, while two thermal resistances at each side of the wall recorded surface temperatures. The collected data were then used to compute the local conductance of the system [11,12]; the experimental results are reported in Table 1.

In Case 1 the conductance over the steel studs is not available due to a failure of the data collecting system. However, it can be supposed, following the behavior of Case 2, that the conductance in this position will be slightly higher than the one at the center of the plasterboard. It is worth noting that, with the configuration of Fig. 1, the metal stud is not in direct contact with the cold wall surface, therefore the expected increase of conductance can be ascribed to the conduction heat transfer through the metal clamps, which represent a point thermal bridge, and the convective heat exchange with the air cavity. Nevertheless, the difference in conductance for Case 2 reveals that the interaction of metal studs and low emissivity surfaces has a far greater importance.

4. Numerical simulation

In order to assess the effect of the steel studs within a range of possible thicknesses of the insulating layer and their interaction with surfaces having different emissivity, a 3D model has been created to accurately represent the heat transfer phenomenon. The model was created using ANSYS Fluent, a software that employs a finite volume discretization and has the ability to consider the coupled effects of radiative and convective heat transfer. The characteristics of the materials used in the model are reported in Table 2.

4.1. Model geometry

In order to speed up the calculation process the geometry was simplified and modeled as in Fig. 2, thus representing a symmetric portion of the wall considering a wall width of 1.24 m. The insulated wall, from cold to hot side, is composed by:

Table 2
Materials' properties.

Material	Density [kg/m^3]	Specific heat [J/(kg K)]	Conductivity [W/(m K)]
Air	1.225	1006.43	0.0242
Brick	1200	840	0.8329
Insulation	30	1450	0.035
Plasterboard	700	1000	0.20
Steel	7800	500	50

- Brick layer: 0.51 m
- Insulation layer: 0.03–0.08 m
- Air cavity: 0.03 m
- Plasterboard: 0.0125 m

Two-dimensional thin layers have been adopted for the horizontal and vertical metal studs, having a thickness of 0.6 mm, in order to effectively consider the heat conduction.

This option allows Fluent to compute heat transfer through these components without generating a true three-dimensional geometry for elements with excessively low thickness. In this way were modeled all the horizontal U-shaped, vertical C-shaped steel studs present in the air cavity and the clamps that intersect the insulating layer all the way to the brick wall.

4.2. Numerical model

In solid domains, steady state energy equation is solved, while in air cavities energy and Navier-Stokes equations are used. Great attention has been employed on the definition of the calculation mesh inside the air cavities formed by the steel studs because of the presence of convective effects due to the temperature differences in the cavity itself. To properly consider the buoyancy-driven nature of air the Boussinesq approximation is used to compute air density inside the cavity. To obtain convergence and reliable results, residuals limits of 10^{-5} were set for continuity, radiation model and velocity in all directions, while a limit of 10^{-10} has been set for the energy equation. First order upwind spatial discretization has been used in fluid domains. A second order upwind scheme has been tested too, however without notable differences, but at the cost of increased computational time.

In order to consider the radiative heat transfer process that occurs in the air cavity the Surface to Surface (S2S) calculation model was set up in Fluent. This model calculates the radiative heat transfer between the cavity surfaces mainly depending on

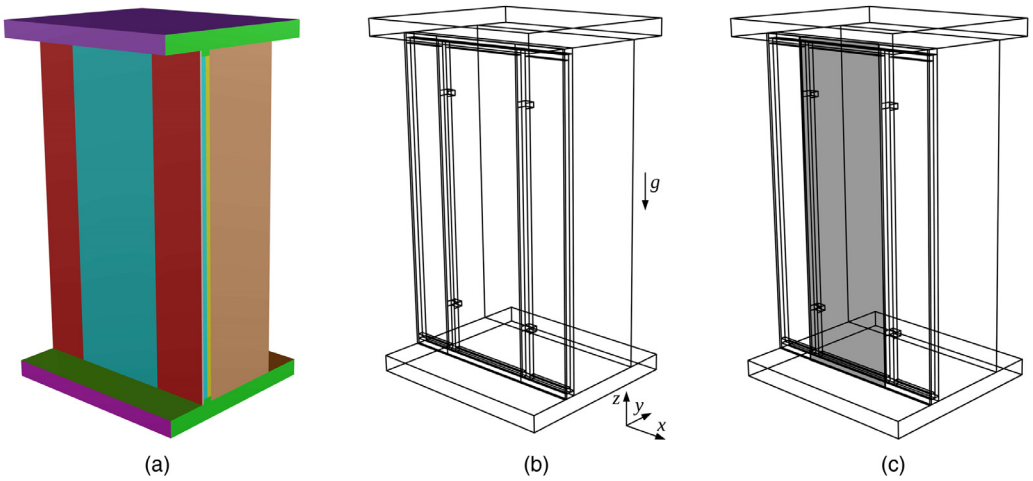

Fig. 2. model geometry (a) steel studs position (b), plasterboard surface used for computing average output values (c).

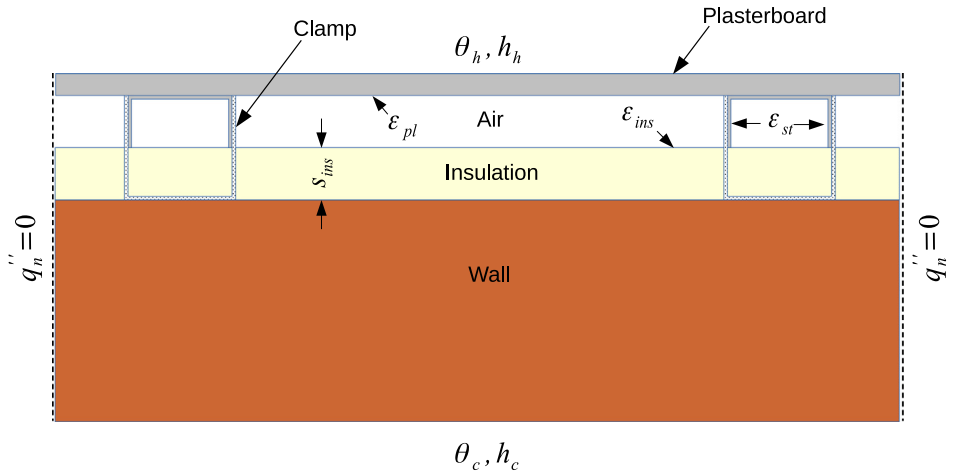

Fig. 3. model boundary conditions.

their size, separation distance, orientation and emissivity. The geometrical part of the model was considered automatically by Fluent through the calculation of the view factors between the surfaces interested by the radiative heat transfer. The emissivity of stud and clamp metal surfaces was set at ε_{st} = =0.23 while the plasterboard's one at ε_{pl} = =0.95. The emissivity of the insulation panel surface facing the air cavity was set at ε_{ins} = 0.95 for not treated surface and ε_{ins} = =0.10 when coated with low-e sheet. The boundary conditions and surface emissivities are also reported in Fig. 3.

In order to reduce the computational time only a periodic sector of the wall has been modelled. therefore, symmetry boundary conditions have been applied to the lateral surfaces shown with dashed lines in Fig. 3. However, the S2S model doesn't behave correctly with symmetric conditions, since near the boundary the radiative contribution of the not modelled surfaces outside the boundary is lost. However, thanks to the reduced thickness of the air cavity, the effect is restricted to a strip near the lateral open boundary. Because of this issue, two vertical studs were inserted in the model to accurately consider the radiative heat exchange in the central portion of the geometry. Therefore, only the central part of the model, delimited by the two vertical studs, as highlighted in Fig. 2c is considered to compute the thermal behavior of the wall.

The presence of hot and cold chambers on the two sides of the wall is modeled through a convective heat transfer wall boundary condition applied to the surfaces as shown in Fig. 3. For the hot chamber a temperature of $\theta_h = 26$ °C with a convective heat transfer coefficient of $h_h = 8.546$ W/(m^2 K) is chosen. The cold side instead is modeled with a temperature of $\theta_c = 5.01$ °C and a convective heat transfer coefficient of $h_c = 14.06$ W/(m^2 K). The heat transfer coefficients have been computed using the experimental data of temperature and specific heat flux obtained at the center of the insulation board where one dimensional heat flux is expected to occur.

4.3. Grid independence test

Before initiating the main simulations, a grid independence test is carried on for a system with low surface emissivity and 3 cm thick insulating layer. The results of three different grids: coarse, medium and fine, were then compared to evaluate the stability of the results. Table 3 reports the values of conductance for clear wall and steel studs positions and Coarse-Medium and Medium-Fine variation.

The conductance is computed using Eq. (1) where q is the heat flux in W/m^2, θ_h and θ_c are the hot and cold chamber temperatures, h_h and h_c are the hot and cold convective coefficients in W/(m^2 K):

$$C = \left[\left(\frac{q}{\theta_h - \theta_c}\right)^{-1} - \frac{1}{h_h} - \frac{1}{h_c}\right]^{-1} \quad (1)$$

Table 3
Grid independence test results.

Grid	Nodes	C_{CW} [W/(m^2 K)]	Var. [%]	C_{st} [W/(m^2 K)]	Var. [%]
Coarse	901,595	0.4194	\	0.6526	\
Medium	2,434,458	0.3990	4.86	0.6466	0.92
Fine	3,146,739	0.3995	0.13	0.6532	0.99

Independence test highlights very low variation between medium and fine grid results, pointing out that the medium grid is precise enough to guarantee reliable results. However, because of similar computation time, the fine grid is chosen to run the numerical simulation to further improve the precision of the results.

4.4. Numerical analysis

First of all, in order to assess the reliability of the 3D model, a simplified geometry having 3 cm of insulation without steel studs was created. This approach allows a direct comparison with the conductance C_{ISO} obtainable using the procedure reported in the EN ISO 6946:2018 standard [13]. About the latter, an iterative calculation is used to evaluate the thermal resistance of an air cavity with various emissivity and homogeneous stratigraphy. The method proposed by the standard is considered to be very reliable, however, as stated by Escudero et al. [14], great attention has to be set on the determination of surface's emissivity. As a matter of fact, Escudero considered an emissivity varying from 0.03 to 0.30 for low-e surfaces to determine air cavity thermal resistance and found that little variation of emissivity value led to considerable variations of the thermal resistance; this effect also became more important with the increase of air gap thickness. Calculations led to a wall conductance of 0.5902 W/(m^2 K) for normal emissivity surfaces and of 0.4540 W/(m^2 K) for low-e solution. At the same time, Fluent model led to values of conductance of 0.5320 W/(m^2 K) and 0.4467 W/(m^2 K) for normal and low-e solutions respectively. It can be noted how the results are quite similar, thus proving the reliability of the Fluent model for a homogeneous stratigraphy of the wall system.

To accurately evaluate the combined effects of the steel studs and air cavity surfaces emissivity variation, different analysis were carried on. To generalize the results, configurations with insulating layer thickness ranging from 3 to 8 cm with 1 cm step were considered. For each insulating panel thickness simulations were carried on considering first high emissivity surfaces only, Case 1, and then with a low-e surface on insulation panel side, Case 2. The combination of parameters led to a total of 12 different simulations.

5. Results

5.1. Output parameters

To evaluate properly the performance of the internal insulation of the wall, the main parameter that has to be considered is the conductance calculated in three significant points. These are the center of the plasterboard where the effect of the steel studs is nearly negligible, the center of one of the steel studs and where the stud connects with the clamp. These three points highlight the variation of the conductance along the geometry of the system. However, the most important output to be considered is the difference between the conductance computed through standard formulas and the numerical conductance weighted on the domain surface highlighted in Fig. 2c, which includes the central part of the plasterboard and one of the steel studs. The analysis allows to evaluate the difference between the declared values usually used on the market, which neglect the effect of metal studs, and the correct value that considers all the components of the internal insulation system.

Table 4
Conductance numerical results.

	C_{cl} [W/(m^2 K)]		C_{st} [W/(m^2 K)]		C_{CW} [W/(m^2 K)]	
s_{ins} (cm)	Case 1	Case 2	Case 1	Case 2	Case 1	Case 2
3	1.01	0.97	0.60	0.65	0.57	0.40
4	0.93	0.90	0.51	0.57	0.49	0.35
5	0.86	0.86	0.45	0.52	0.42	0.32
6	0.79	0.79	0.40	0.47	0.37	0.29
7	0.73	0.74	0.36	0.44	0.34	0.27
8	0.69	0.71	0.34	0.47	0.31	0.25

About the Fluent results it has been noted that with low values of emissivity the solution does not reach the convergence limits for the energy equation but it oscillates around residuals of 10^{-9}. This is due to the formation of slight periodic air movements in the cavity that cannot be resolved in a stationary analysis. However, a time dependent simulation showed that this behavior does not affect the reliability of the results, therefore, in order to reduce the required time, the computation has been performed in a steady state condition only.

5.2. Simulation results

Table 4 presents the results of the simulations carried on with Fluent for cases with insulating layer thickness s_{ins} varying from 3 to 8 cm. The reported values are detected at mid height of the plasterboard, but in different locations: at the middle of the plasterboard C_{CW}, identified as a clear wall position, in correspondence of the steel stud C_{st}, an additional location has been considered at the connection between the steel stud and the clamp that fixes it to the brick layer C_{cl}. Table 4 reports the results for both cases by changing the surface emissivity of the insulation panel facing the air cavity.

It can be noted that, as expected, the highest value of conductance is detected at the connection between the clamps and the studs, while the lowest on the plasterboard, having an intermediate value on the mid-height point of the steel stud. Then it can be noted that, as expected, increasing the thickness of the insulation leads to an overall reduction of the values of the conductance.

The inspection of Table 4 reveals that the conductance at clamp position does not significantly change between Case 1 and Case 2, the higher values respect the clear wall ones can be justified by the presence of a point thermal bridge going from the plasterboard to the underneath cold wall by means of conductance heat transfer along the clamps. Quite different results are obtained for the conductance computed in correspondence of the vertical studs: for Case 1 C_{st} values are always lower than the values obtained for Case 2, it is interesting to note how the difference raises with increased insulation layer thickness.

An important result to account for is the tendency of the conductance to increase in stud C_{st} and stud-clamp C_{cl} positions when lowering the emissivity of the insulating surface of the air cavity.

In Figs. 4 and 5 conductance and temperature's trends are reported along the z–axis of the model. The main feature noted is that these trends show disturbances in correspondence of the hor-

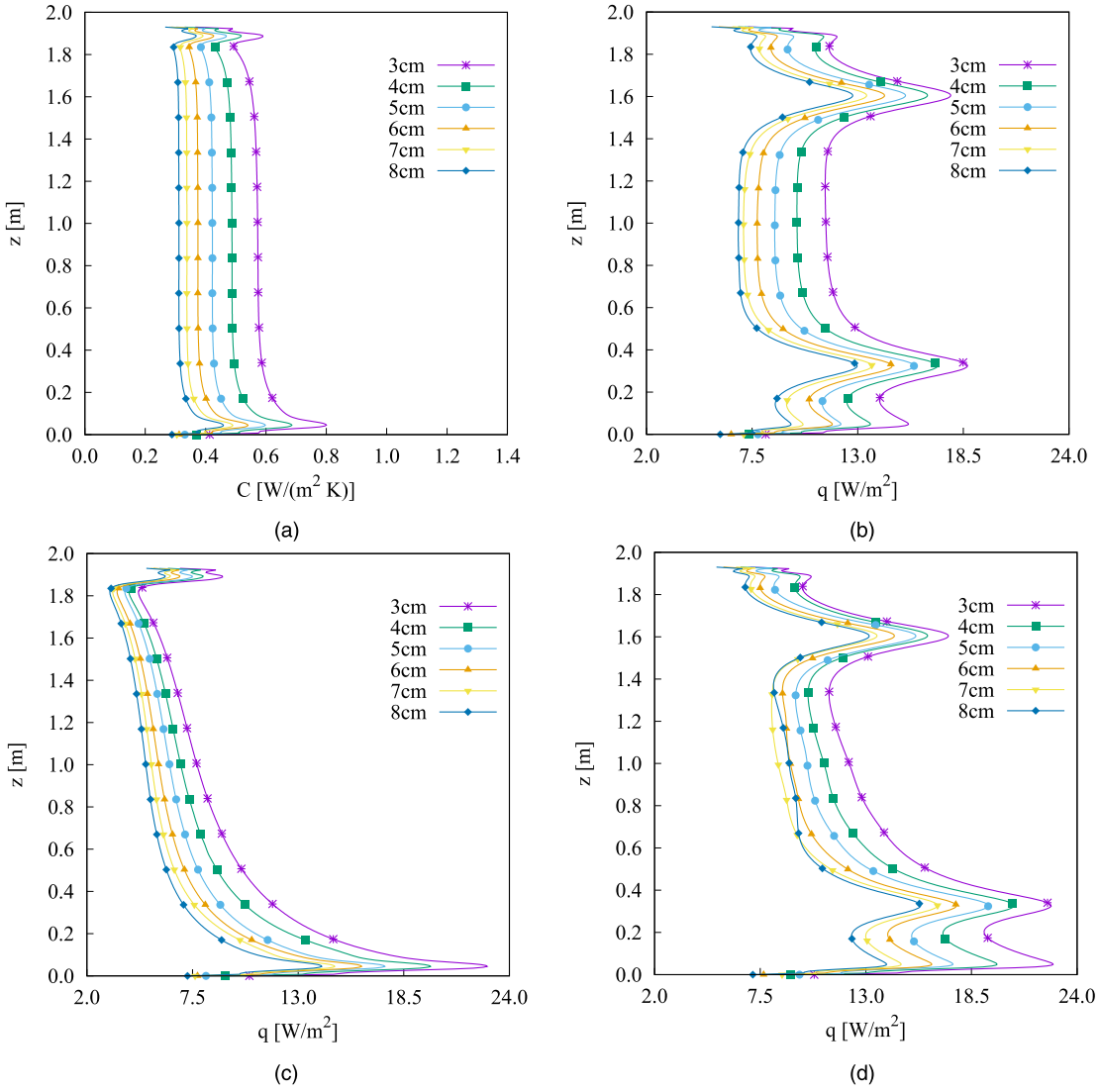

Fig. 4. conductance trend along z-axis. On the center of the plasterboard Case 1 (a) and Case 2 (c) In correspondence of the stud Case 1 (b) Case 2 (d).

izontal studs for both plasterboard and steel stud distributions and at the clamps positions only for the second ones. It can be noted how the presence of the clamps has a way greater influence on the system than the horizontal U-shaped supporting frames, since the clamps create a thermal bridge all the way to the underneath wall, while the horizontal U-shaped studs behave has linear thermal bridges up to the internal insulation panel surface.

The inspection of Figs. 4 and 5 reveals that the presence of low emissivity surfaces increases the disturbance caused by studs and clamps, furthermore temperature and conductance vertical distribution are quite different from each other. The high emissivity case shows a rather uniform distribution, while in the low-e case the distribution appears tilted, suggesting a different behavior of heat transfer inside the cavity for standard and low-e cases.

5.3. Heat transfer inside air cavity

The vertical distribution of temperature and conductance reported in Figs. 4 and 5 suggests that the convection is stronger in Case 2 than in Case 1. It is expected that temperature difference between air gap surfaces, the hot one formed by the plasterboard and the cold one by the insulation panel, generates a circulation flow inside the air gap typical of differentially heated cavities, where the higher the temperature difference, the stronger the air circulation that is generated. Fig. 6 reports the vertical distribution of the temperature difference between cardboard and insulation panel surfaces computed at the mid of the air cavity for both cases end for the different insulation panel thicknesses. Case 2 shows a far greater temperature difference than Case 1 due to the presence of the low-e layer and a lower temperature on the insulation panel surface. With a greater temperature difference, a stronger air circulation occurs in the cavity, Table 5 reports the maximum and minimum velocities registered in the air gap for both cases; it can be noted how the Case 2 always shows higher velocities than the ones of Case 1. The stronger recirculating region in the air cavity

Table 5
maximum and minimum velocities in air gap.

	Case 1		Case 2	
s_{ins} [cm]	max w [m/s]	min w [m/s]	max w [m/s]	min w [m/s]
3	0.0452	−0.0445	0.0963	−0.0831
4	0.0380	−0.0475	0.0859	−0.0740
5	0.0324	−0.0470	0.0807	−0.0734
6	0.0300	−0.0483	0.0781	−0.0659
7	0.0259	−0.0470	0.0711	−0.0648
8	0.0257	−0.0458	0.0727	−0.0594

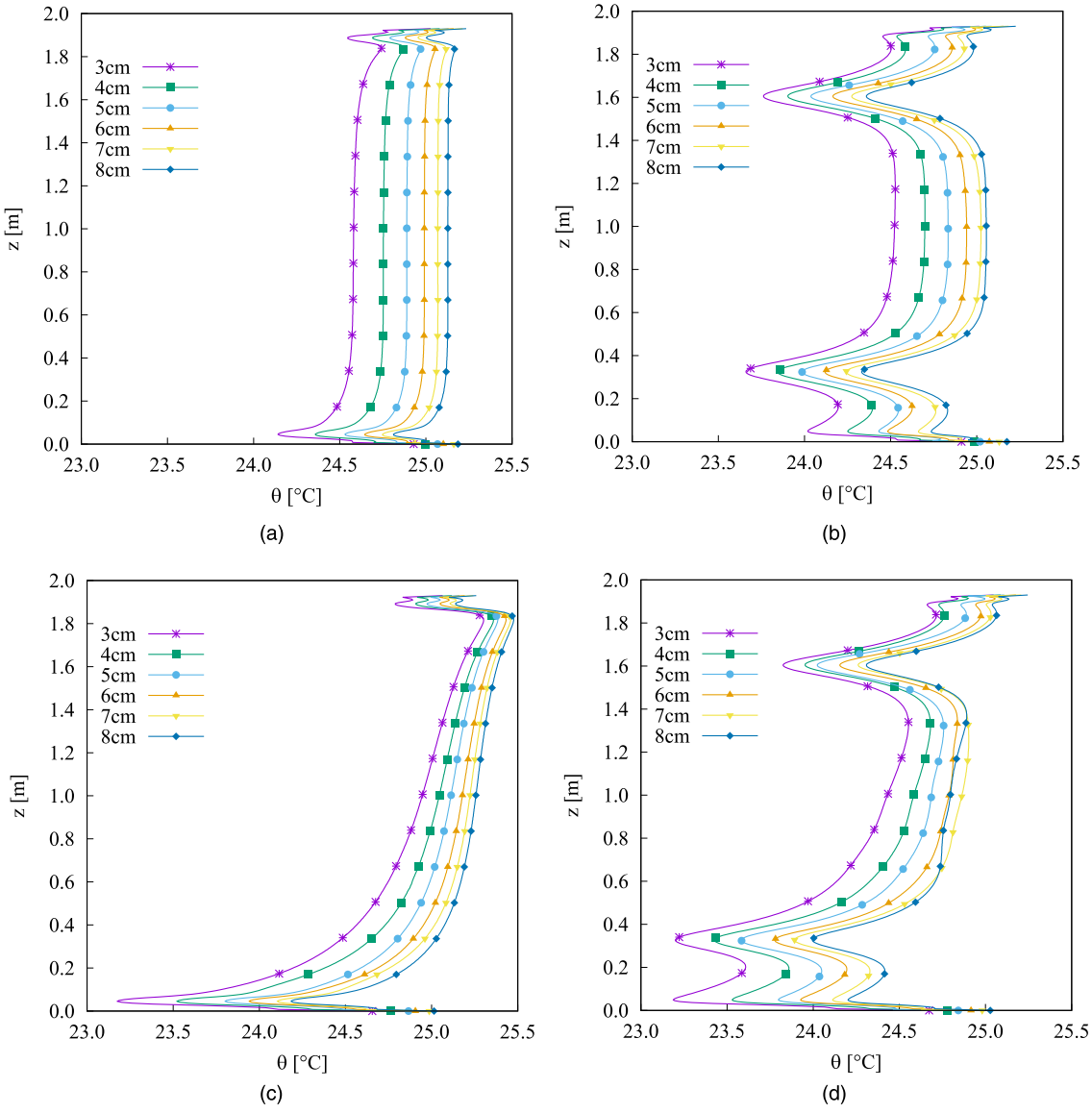

Fig. 5. temperature trend along z-axis. On the center of the plasterboard Case 1 (a) and Case 2 (c) In correspondence of the stud Case 1 (b) Case 2 (d).

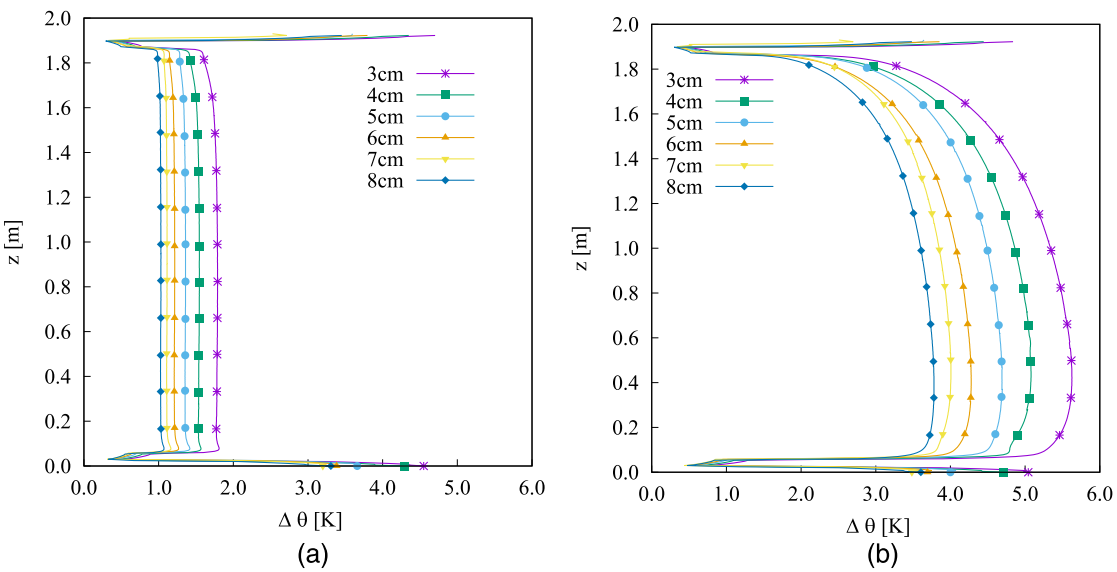

Fig. 6. temperature difference along mid-air cavity for different insulation thicknesses Case 1 (a) Case 2 (b).

Table 6
Heat exchange between studs and air gap.

s_{ins} [cm]	Case 1 [W]	Case 2 [W]	Var. [%]
3	0.124	0.198	59.68
4	0.101	0.179	77.23
5	0.072	0.147	104.17
6	0.053	0.116	118.87
7	0.052	0.115	121.15
8	0.032	0.075	134.38

Table 7
Comparison between standard and average conductance values.

	Case 1			Case 2		
s_{ins} [cm]	C_{ISO} [W/(m^2 K)]	C_{AVG}	E_{ISO} [%]	C_{ISO} [W/(m^2 K)]	C_{AVG}	E_{ISO} [%]
3	0.590	0.591	0.23	0.473	0.511	7.97
4	0.505	0.508	0.56	0.414	0.450	8.72
5	0.441	0.443	0.41	0.369	0.403	9.17
6	0.392	0.397	1.22	0.332	0.367	10.61
7	0.353	0.359	1.72	0.302	0.341	12.98
8	0.320	0.333	4.10	0.278	0.322	15.77

influences also the heat transfer exchanged between the sides of the vertical studs facing the air cavity, that are reported in Table 6. Vertical studs exchange with the air cavity a greater heat flux in Case 2 than in Case 1 due to the stronger air recirculation, therefore increasing also the heat flux and conductance reported at stud position as highlighted in Fig. 4.

5.4. Heat exchange of the overall insulation system

The inspection of Fig. 4 highlights the requirement to include the stud's effect in the computation of the overall insulation and the presence of a possible error when this effect is discarded; this happen typically when the mean conductance is obtained using clear wall values only.

The numerical computation of the heat flux through the surface highlighted in Fig. 2c allows the definition of an average conductance of the wall C_{AVG}, which correctly considers the presence of metal studs.

Therefore, a result to account for is the comparison between the values obtained applying the international standards in computing conductance, C_{ISO}, and the ones obtained considering the average value of conductance, C_{AVG}. To evaluate the difference between the results, the error respect the international standard value is introduced with Eq. (2). However, differences also occur between the results obtained from a numerical computation of a clear wall for the simplified geometry and the average ones, therefore Eq. (3) presents the error between the average conductance C_{AVG} and the numerical computed clear wall value C_{CW}.

$$E_{ISO} = \frac{C_{ISO} - C_{AVG}}{C_{ISO}} \times 100 \tag{2}$$

$$E_{CW} = \frac{C_{CW} - C_{AVG}}{C_{CW}} \times 100 \tag{3}$$

In Table 7, the influence of both the steel studs, surfaces emissivity and their interaction can be appreciated. With normal values of emissivity, the error that occurs disregarding the effect of the steel studs varies in a range between ≅0.20% and ≅4.00% showing an increasing trend with the insulation thickness. Considering instead the low-e solution, the error grows consistently reaching a value between ≅8.00% and ≅16.00%. A common behavior is evident: the more the system is insulated, regardless of the insulation method, the more the influence of the steel studs becomes evident and influential.

Table 8 reports the difference between clear wall and average values obtained using Fluent. This comparison has been done to highlight the different behavior of the two situations if both are computed through numerical simulation. In this manner some simplifications introduced by the standard to represent the heat transfer phenomena are bypassed. Results show that in this case differences between clear wall and average values are even greater, ranging from ≅3.20% to ≅7.00% for Case 1 and from ≅25.80% to ≅28.00% for Case 2.

Table 8 inspection then shows that using a numerical method, but disregarding the presence of the steel studs, could lead to a performance evaluation error up to a remarkable 28%.

As a final remark some guidelines for designers can be drawn. In order to reduce heat losses into refurbished buildings internal insulation systems can be applied, but with carefulness. The formation of air gaps in the insulation structure isolates the metal studs from the cold underneath wall reducing the thermal bridge effect, for high emissivity surfaces the stud effect is rather low with a maximum value of 4.1%. The adaption of low-e surfaces is a practical and economical way to increase the insulation effect. However, in this case the effect of metal structures cannot be disregarded since the error can be up to 28%. However, also if the effect of metal studs is taken into account the use of low-e surfaces is beneficial in decreasing the overall conductance of the wall since the C_{AVG} values for Case 2 are always lower than the ones computed in Case 1 as reported in Tables 7 and 8.

Conclusions

This paper presented a methodology for the correct evaluation of internal insulation systems for building refurbishment. The internal insulation system features an insulating layer positioned on the wall, an air gap, required to accommodate structural metal studs for supporting the finishing plasterboard, and the plasterboard itself. Since the air gap in the structure contributes to the heat exchange with both convection and radiation heat transfer, two cases have been analyzed: the former with high emissivity

Table 8
Comparison between clear wall and average conductance values.

	Case 1			Case 2		
s_{ins} [cm]	C_{CW} [W/(m^2 K)]	C_{AVG} [W/(m^2 K)]	E_{CW} [%]	C_{CW} [W/(m^2 K)]	C_{AVG} [W/(m^2 K)]	E_{CW} [%]
3	0.573	0.591	3.28	0.399	0.511	28.00
4	0.487	0.508	4.21	0.353	0.450	27.66
5	0.422	0.443	4.88	0.320	0.403	25.79
6	0.374	0.397	6.00	0.290	0.367	26.68
7	0.338	0.359	6.24	0.270	0.341	26.46
8	0.312	0.333	6.88	0.255	0.322	26.41

surfaces the latter with a low emission layer installed on the cold side of the gap. Different insulation layer thicknesses have been analyzed ranging from 3 cm to 8 cm. A numerical model has been first validated using experimental results obtained using heat flow meter measures in a controlled setup, then used to evaluate the effect of low emission coatings in the air gap and the effect of the interaction of structural metal studs into the air gap layer. The results revealed that for the high emissivity case the impact of the metal studs is negligible, however the use of low emissivity coatings changes dramatically the panorama. Although the use of low emissivity layers is beneficial, increasing the thermal resistance of the system for clear wall values, the interaction with the metal studs decreases the effectiveness. Taking into account the metal studs the overall thermal conductance shows an increase of up to 28.00%. The results show that the use of clear wall values for evaluating the thermal resistance of an internal insulation system may lead to an overestimation of the energy savings for a refurbished building, especially if low emissivity layers are inserted in order to increase the overall thermal resistance.

Funding

This work was supported by University of Trieste with FRA 2015 grant.

Declaration of Competing Interest

We wish to confirm that there are no known conflicts of interest associated with this publication and there has been no significant financial support for this work that could have influenced its outcome.

Acknolewdgments

Authors thank the Edilmaster building school of Trieste for the support in setting up the experimental chamber.

References

[1] G. Baldinelli, A methodology for experimental evaluations of low-e barriers thermal properties: field tests and comparison with theoretical models, Build. Environ. 45 (April (4)) (2010) 1016–1024, doi:10.1016/j.buildenv.2009.10.009.

[2] A. Joudi, H. Svedung, M. Rönnelid, Energy efficient surfaces on building sandwich panels – A dynamic simulation model, Energy Build. 43 (April (9)) (2011) 2462–2467, doi:10.1016/j.enbuild.2011.05.026.

[3] H.H. Saber, Investigation of thermal performance of reflective insulations for different applications, Build. Environ. 52 (June 2012) 32–44, doi:10.1016/j.buildenv.2011.12.010.

[4] S. Fantucci, V. Serra, Investigating the performance of reflective insulation and low emissivity paints for the energy retrofit of roof attics, Energy Build. 182 (January) (2019) 300–310, doi:10.1016/j.enbuild.2018.10.003.

[5] M. Ibrahim, L. Bianco, O. Ibrahim, E. Wurtz, Low-emissivity coating coupled with aerogel-based plaster for walls' internal surface application in buildings: energy saving potential based on thermal comfort assessment, J. Build. Eng. 18 (July) (2018) 454–466, doi:10.1016/j.jobe.2018.04.008.

[6] A. Joudi, H. Svedung, M. Cehlin, M. Rönnelid, Reflective coatings for interior and exterior of buildings and improving thermal performance, Appl. Energy 103 (March) (2013) 562–570, doi:10.1016/j.apenergy.2012.10.019.

[7] J.C. Cook, D.W. Yarbrough, K.E. Wilkes, Contamination of reflective foils in horizontal applications and the effect on thermal performance, Conf. Proc. ASHRAE Trans. 5 (Part 2) (1989) 677–681.

[8] J. Kosny, J.E. Christian, Thermal evaluation of several configurations of insulation and structural materials for some metal stud walls, Energy Build. 22 (2) (1995) 157–163, doi:10.1016/0378-7788(94)00913-5.

[9] E. De Angelis, E. Serra, Light steel-frame walls: thermal insulation performances and thermal bridges, Energy Proc. 45 (2014) 362–371, doi:10.1016/j.egypro.2014.01.039.

[10] N. Soares, P. Santos, H. Gervàsio, J.J. Costa, L. Simoes Da Silva, Energy efficiency and thermal performance of lightweight steel-framed (LSF) construction: a review, Renew. Sustain. Energy Rev. 78 (October) (2017) 194–209, doi:10.1016/j.rser.2017.04.066.

[11] M. Manzan, E. Zandegiacomo De Zorzi, W. Lorenzi, Experimental and numerical comparison of internal insulation systems for building refurbishment, Energy Proc. 82 (December) (2015) 493–498, doi:10.1016/j.egypro.2015.11.853.

[12] M. Manzan, E. Zandegiacomo De Zorzi, W. Lorenzi, Numerical simulation and sensitivity analysis of a steel framed internal insulation system, Energy Build. 158 (January) (2018) 1703–1710, doi:10.1016/j.enbuild.2017.11.069.

[13] UNI EN ISO 6946:2018. Componenti ed elementi per edilizia – Resistenza termica e trasmittanza termica–Metodi di calcolo. 2018.

[14] C. Escudero, K. Martin, A. Erkoreka, I. Flores, J.M. Sala, Experimental thermal characterization of radiant barriers for building insulation, Energy Build. 59 (April) (2013) 62–72, doi:10.1016/j.enbuild.2012.12.043.